Virology **275,** 249–257 (2000)
doi:10.1006/viro.2000.0532, available online at http://www.idealibrary.com on IDEAL®

RAPID COMMUNICATION

Packaging of Tobacco Mosaic Virus Subgenomic RNAs by Brome Mosaic Virus Coat Protein Exhibits RNA Controlled Polymorphism

Yoon Gi Choi and A. L. N. Rao[1]

Department of Plant Pathology, University of California, Riverside, California 92521-0122

Received June 23, 2000; returned to author for revision July 7, 2000; accepted July 12, 2000

The coat protein (CP) of icosahedral *Brome mosaic virus* (BMV) was expressed from a genetically engineered rod-shape *Tobacco mosaic virus.* Molecular characterization of the progeny recovered from symptomatic plants revealed that BMV CP selectively packaged the three subgenomic RNAs of the hybrid virus into two differently sized icosahedral virus-like particles (VLPs). The smaller VLPs packaged only the two smaller subgenomic RNAs. Additional *in vitro* reassembly assays with BMV CP subunits and transcripts of hybrid subgenomic RNAs further demonstrated that the ability of BMV capsids to display polymorphism is not dependent on the RNA size alone and appears to be controlled by some other feature(s) of the genetically engineered RNA.

A variety of specific RNA–protein interactions are recognized to play an important role in the infection cycle of a wide spectrum of RNA viruses infecting plants, insects, animals, and humans. One such interaction results in the assembly of infectious ribonucleocapsids (virions). It is envisioned that this important phase is initiated by specific sequence- and/or structural-dependent interactions between viral coat protein and RNA in order to ensure that a majority of the virions contain exclusively viral RNA. Two RNA viruses of plants, an isometric *Brome mosaic virus* (BMV; *1*) and a rod-shape *Tobacco mosaic virus* (TMV; *3*) exhibit similar replication mechanisms but are distinct in other properties. BMV is a tripartite virus. The largest two genomic RNAs 1 (3224 nt) and 2 (2865 nt) encode nonstructural proteins that are required for viral RNA replication (*2*). The 5′ ORF of the third genomic RNA3 (2117 nt) encodes a movement protein (MP) while the 3′ proximal ORF encoding the coat protein (CP) is expressed via subgenomic RNA4 (884 nt; *1*). TMV is a monopartite virus (*3*). The first two ORFs, encoding replicase proteins, are translated directly from the genomic RNA; the 30-kDa movement protein and 17-kDa coat protein are translated from two independent subgenomic mRNAs that are 3′ coterminal (*3*). In addition, another subgenomic mRNA containing an ORF for a 54-kDa protein that encompasses the read-through region of replicase ORF has been isolated from infected tissue, although no protein has been detected (*4*).

Despite similarities in replication mechanisms, TMV and BMV differ significantly in their host range and most importantly in packaging genomic and subgenomic RNAs. In BMV, the three genomic and the single subgenomic CP mRNA are encapsidated into three separate particles of identical shape and size with $T = 3$ icosahedral symmetry: genomic RNAs 1 and 2 are packaged individually into separate particles whereas RNAs 3 and 4 are thought to be copackaged into a single particle (*5*). The majority of *tobamoviruses* having the origin of assembly sequence (OAS) in the MP cistron package detectable amounts of genomic RNA but only the MP subgenomic RNA is detected upon enrichment of the high-speed supernatant (*6*). *Sunn-hemp mosaic virus* having OAS in the CP cistron has been shown to package genomic RNA into normal-size rods and detectable levels of subgenomic RNAs of MP and CP into shorter rods (*6, 7*).

In this study, we engineered a TMV-based vector to express BMV CP *in vivo* via an independent subgenomic RNA. Characterization of virus-like particles (VLPs) recovered from infection resulting from the inoculation of the TMV hybrid virus revealed a previously unrecognized feature associated with BMV CP, i.e., packaging of three subgenomic RNAs derived *in vivo* from TMV hybrid replication into two distinct-size VLPs. To the best of our knowledge, this is the first report of TMV subgenomic RNAs being packaged by a nontobamovirus coat protein. It is anticipated that the system described here will have important ramifications in understanding the sequence and/or structural features dictated by a genetically engineered RNA in controlling virion polymorphism in viruses with icosahedral symmetry.

[1] To whom correspondence and reprint requests should be addressed. Fax: (603) 590-6673. E-mail: A.RAO@ucr.edu.

0042-6822/00 $35.00

Results and Discussion. Characteristics of TMV hybrid vector 30B-BCP designed to express BMV CP. The characteristics of a genetically engineered TMV-based vector (p30B; Fig. 1A) for foreign gene expression has been described previously (*8, 9*). To express wild-type (wt) BMV CP from this TMV-based vector, a variant clone referred to as p30B-BCP was constructed (Fig. 1B). It is anticipated that infections resulting from inoculation of 30B-BCP transcripts will result in the synthesis of three subgenomic RNAs and BMV CP is expected to be exclusively translated from subgenomic RNA 3 (SgRNA 3) of 842 nt (Fig. 1C). Independent transfection of protoplasts with 30B-BCP transcripts resulted in efficient synthesis of BMV CP when subjected to Western blot analysis using antisera specific for BMV CP (data not shown).

Infections of Whole Plants with 30B-BCP. Chenopodium quinoa is a common permissive host for TMV and BMV with distinguishable symptom phenotypes. Both TMV U1 and BMV infection result in the induction of chlorotic local lesions that expanded with time yielding large chlorotic blotches (Fig. 1D). However, the uninoculated upper leaves of plants inoculated with BMV, but not TMV U1, display systemic mottling and leaf distortion (*10*). Independent inoculation with *in vitro* synthesized transcripts of 30B-BCP to *C. quinoa* plants resulted in the induction of chlorotic local lesions that turned necrotic with time (Fig. 1D). Like wt TMV, none of these plants displayed any visible symptoms on uninoculated upper leaves and no hybridization signal was detected when total RNA from these symptomless leaves was probed with riboprobes complementary to either the TMV U1 CP ORF sequence or the 3′ tRNA-like region of BMV RNAs (data not shown).

Selective Packaging of 30B-BCP Subgenomic RNAs by BMV CP into Two Differently Sized VLPs. TMV infection can spread cell-to-cell without CP (*11*) while BMV infection requires both movement protein and encapsidation competent CP (*10, 12*). Since BMV CP has been shown to exhibit a high degree of specificity in packaging both *in vitro* and *in vivo* (*13, 14*) and because of the fact that the genomic RNA of 30B-BCP is too large to be encapsidated by BMV CP into icosahedral virions of 28 nm, no virion formation is expected. Therefore the induction of visible symptom phenotypes in *C. quinoa* must have resulted from cell-to-cell movement of 30B-BCP mediated by TMV MP only. To confirm the assumption that no virions are assembled from BMV CP subunits in these infections, virions were purified from symptomatic leaves using a buffer system optimum for BMV. Contrary to our assumption, electron microscopic examination of a negatively stained partially purified preparation revealed the presence of icosahedral virus-like particles with two distinct sizes: approximately 90% of VLPs measured 28 nm in diameter and are indistinguishable from those of wt BMV virions (hereafter these will be referred to as VLP^{28}), whereas the remaining 10% measured 22–24 nm in diameter (hereafter these will be referred to as VLP^{22}; Fig. 2A). Western blot analysis of CP isolated from these purified VLPs confirmed the expected BMV parental origin, as evidenced by specific interactions with anti-BMV CP (Fig. 2B). To verify that VLPs detected in these purified preparations are not due to contamination with wt BMV, RNA was isolated from nuclease-resistant purified VLP preparations and duplicate Northern blots containing the virion RNA were hybridized with riboprobes complementary to a highly conserved 3′ tRNA-like region of BMV RNAs. Absence of any detectable hybridization signal by these specific riboprobes (Fig. 2C) confirmed that infection of 30B-BCP was not due to contamination with wt BMV. Likewise, the absence TMV CP (Fig. 2B) and TMV RNA (Fig. 2C) in Western and Northern blots, respectively, confirmed that symptom induction in *C. quinoa* by 30B-BCP is not due to wt TMV contamination.

Bromovirus CP subunits cannot assemble into empty virions *in vivo* since they are stabilized by RNA–protein interactions (*5, 15*). Therefore, the two distinct-size VLPs assembled from BMV CP must have packaged some RNA. To analyze the nucleic acid profile in these VLPs, multiple Northern blots containing total nucleic acid preparations extracted from symptomatic inoculated leaves of *C. quinoa* as well as RNA recovered from nuclease resistant VLPs of 30B-BCP were produced. Results of these hybridization experiments are summarized in Fig. 3. Hybridization of a Northern blot containing total nucleic acid preparations of TMV U1 and 30B-BCP

FIG. 1. Characteristics and genome organization of TMV-based hybrid vectors designed to express foreign genes. (A) Schematic representation of a TMV-based expression vector (p30B), assembled from parts of TMV U1 and TMGMV U5 (*9*), to engineer foreign genes between *Pac*I and *Xho*I restriction sites. The 126- and 183-kDa proteins constitute viral replicase proteins and the 30-kDa protein is the movement protein. In this vector, the 3′ proximal region contains the entire CP gene sequence and the 3′ nontranslated region from TMGMV U5. SGP denotes the location of the subgenomic promoters. (B) p30B-BCP is characterized by having BMV CP ORF between *Pac*I and *Xho*I restriction sites. The 3′ noncoding region is derived from TMV U1 (see Materials and Methods). The bars above 54-kDa ORF, 30-kDa ORF, and BMV CP ORF represent the regions used to synthesize riboprobes. Three subgenomic RNAs (SgRNA 1, 2, and 3) derived from the replication of 30B-BCP *in vivo* are shown. Filled circles at the 5′ end and the clover-leaf-like structures at the 3′ end represent the cap and tRNA-like structures, respectively. The predicted sizes of genomic and subgenomic RNAs of the hybrid virus are shown to the left. (C) Schematic representation of transcriptional plasmids for synthesizing *in vitro* transcripts corresponding to each of the three subgenomic RNAs of 30B-BCP used for *in vitro* reassembly assays. The characteristics of pT7B4 are as described previously (*15*). At the 5′ end of each plasmid, an arrow represents the position of T7 RNA polymerase promoter. T7 promoter sequences and viral sequences are shown in lower- and uppercase letters, respectively. (D) Symptom phenotypes induced by each parental virus and the hybrid 30B-BCP on *Chenopodium quinoa* are shown. Leaves were photographed 5 days postinoculation.

A p30B

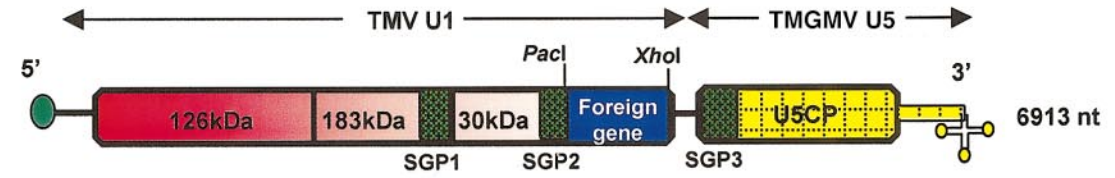

B p30B-BCP

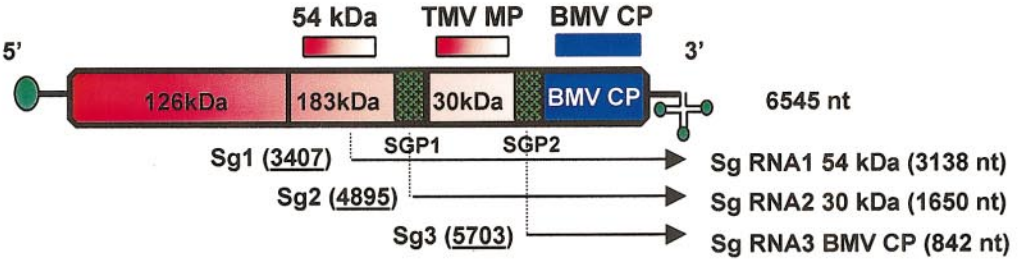

C Transcriptional plasmids for *in vitro* reassembly assays

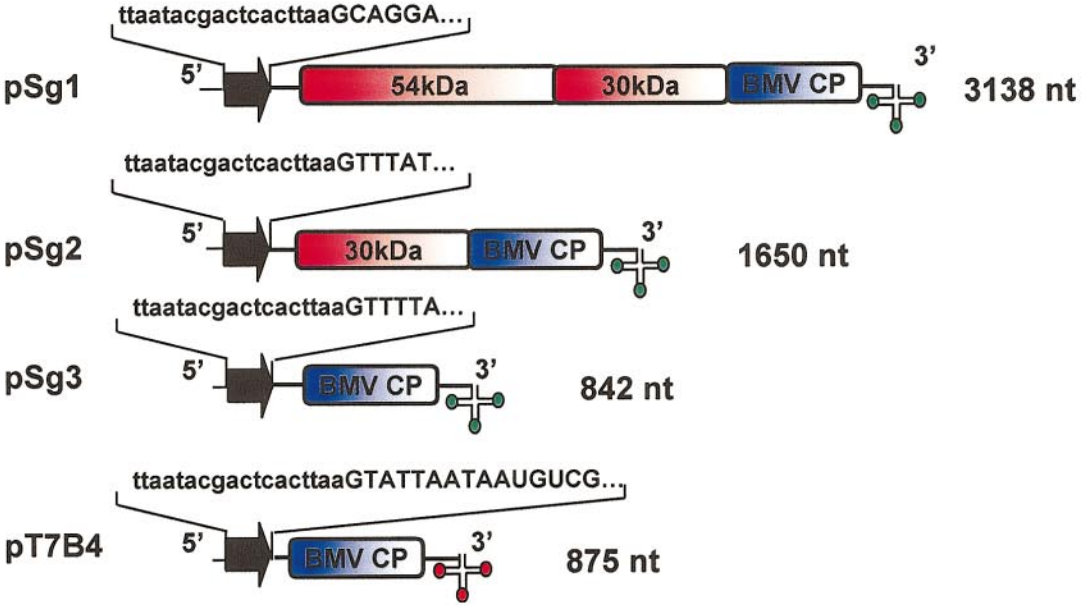

D Symptom phenotypes on *Chenopodium quinoa*

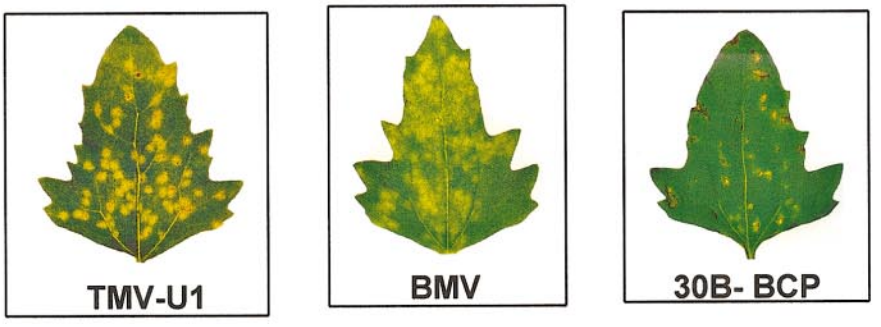

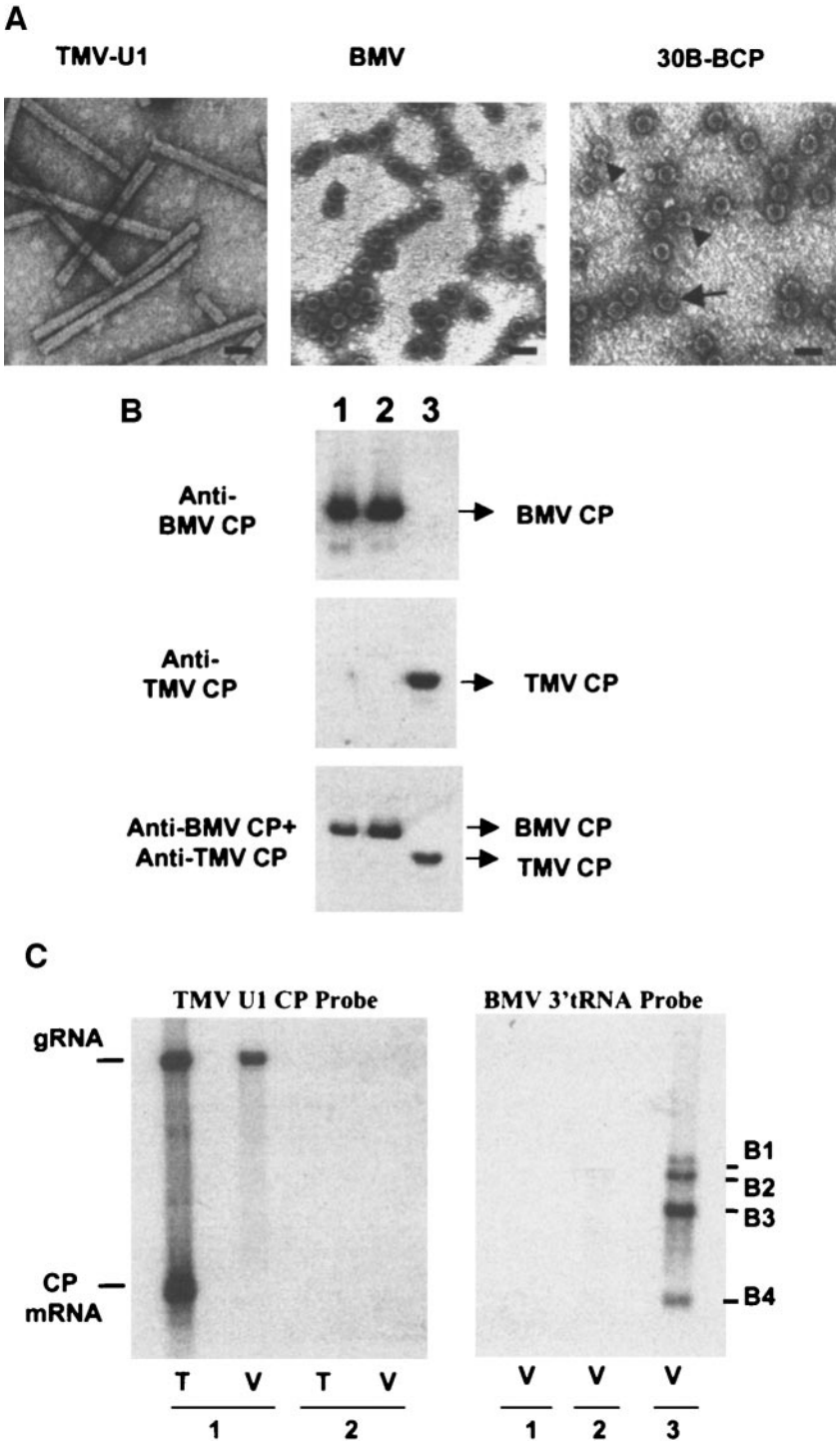

FIG. 2. Characteristics of parental and hybrid 30B-BCP progeny. (A) Electron micrographic images showing virions of wt TMV U1, wt BMV, and virus like particles (VLPs) of hybrid 30B-BCP purified symptomatic inoculated leaves of *C. quinoa.* Virion preparations were negatively stained with uranyl acetate and photographed under a Hitachi electron microscope. Arrow indicates normal size VLPs and arrowhead indicates smaller size VLPs. Bar = 50 nm. (B) Western blot analysis of CP. Purified virions of wt BMV (lane 1), hybrid 30B-BCP (lane 2), and wt TMV U1 (lane 3) were suspended in SDS–PAGE sample buffer, denatured by boiling for 5 min, and subjected to multiple gels of 14% polyacrylamide gels. After the proteins were transferred to a nitrocellulose membrane, each blot was probed with either anti-BMV CP or anti-TMV CP or a mixture containing both antisera and detected with an enhanced chemiluminescence kit (Amersham). The positions of BMV CP and TMV CP are indicated to the left. (C) Northern blot analysis of either total nucleic acid (T) or virion RNA (V) preparations recovered from symptomatic leaves of *C. quinoa* of samples (1) wt TMV U1; (2) 30B-BCP; and (3) wt BMV. Approximately 5 μg of total nucleic acid and 100 ng of virion RNA preparations were denatured with glyoxal, fractionated on 1% agarose gel, and electrophoretically transferred to nylon membranes. Each blot was hybridized with the indicated ^{32}P-labeled riboprobes. The positions of TMV genomic RNA (gRNA) and the CP mRNA are shown to the left. The positions of three BMV genomic RNAs (B1, B2, and B3) and a single subgenomic RNA (B4) are shown to the right.

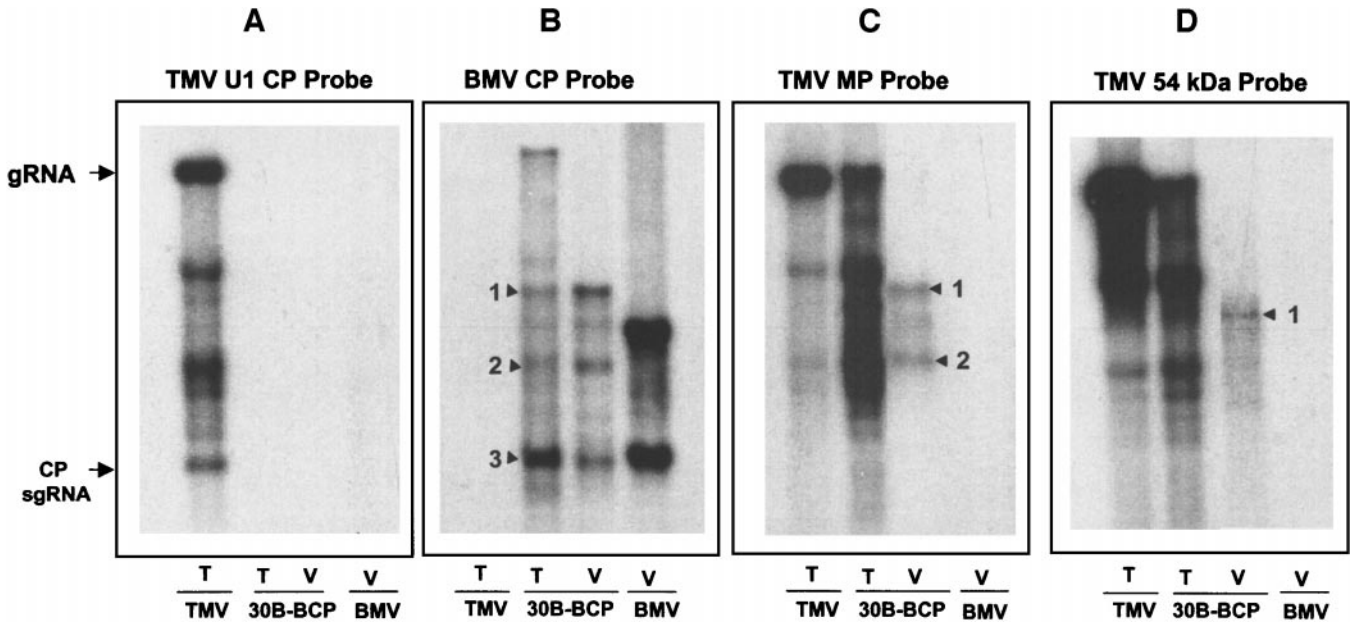

FIG. 3. Characterization of RNAs recovered from VLPs of 30B-BCP. Northern blot analysis of total nucleic acid (T) and RNA from nuclease resistant VLPs of 30B-BCP (V) recovered from symptomatic systemic leaves of *C. quinoa.* Sample preparation and electrophoretic conditions are as described under Fig. 2. Each blot was hybridized with the indicated ^{32}P-labeled riboprobes. In A, the positions of genomic and CP mRNA of wt TMV U1 are indicated. In B–D, the positions of three subgenomic RNAs (Fig. 1A; shown as 1, 2, and 3, respectively) packaged into VLPs recovered from 30B-BCP infection are indicated by arrowheads.

and virion RNA of 30B-BCP and wt BMV with a riboprobe complementary to TMV U1 CP resulted in the detection of only TMV U1 progeny RNA (Fig. 3A). By contrast, hybridization of duplicate Northern blots with a riboprobe complementary to BMV CP ORF (Fig. 3B) revealed unexpected profiles. This riboprobe detected four major RNA species with expected molecular weights in the total nucleic acid preparations of 30B-BCP (Fig. 3B): a slower migrating genomic RNA and three faster migrating subgenomic RNAs (SgRNAs 1–3; Fig. 1B). Hybridization of virion RNA of 30B-BCP with this probe detected only the three SgRNAs but not the genomic RNA (Fig. 3B). The identity of each of the three subgenomic RNAs was further confirmed by hybridizing with riboprobes specific for TMV MP ORF (detects SgRNA1 and 2 only; Fig. 3C) and 54-kDa ORF (detects only SgRNA1; Fig. 3D). These results demonstrate that BMV CP subunits derived from 30B-BCP selectively packaged all three subgenomic RNAs into two distinct VLPs (Figs. 3B–3D).

Three Subgenomic RNAs of 30B-BCP are Distributed Differentially into Two Distinct-Size VLPs. Sucrose density gradient analysis of partially purified high-speed virus pellet of 30B-BCP revealed fast, medium, and slow sedimenting peaks (Fig. 4A). VLPs constituting each peak were fractionated and examined under an electron microscope. Fractions constituting the medium and fast sedimenting peaks contained a homogeneous population of VLP^{28} and VLP^{28H}, respectively (Fig. 4B), while those of the slower sedimenting peak contained a homogeneous population of VLP^{22} (Fig. 4B). This polymorphism associated with 30B-BCP infection was highly reproducible and consistently detected in at least four independent experiments. Although VLPs constituting the medium and slower sedimenting peaks were reproducibly recovered from several experiments, those constituting the faster sedimenting peak (i.e., VLP^{28H}) were recovered only in freshly harvested infected material. Additional stability experiments showed that these virions are unstable and rapidly degraded upon storage at 4°C (data not shown).

In order to verify the virion RNA profiles, fractions constituting each of the three peaks were concentrated following density gradient fractionation and RNA was subjected to Northern blot analysis (Fig. 4C). VLP^{28} recovered from medium sedimenting peak contained all three subgenomic RNAs whereas VLP^{22} recovered from slower sedimenting peak contained only SgRNAs 2 and 3 (Fig. 4C). Interestingly, SgRNA 1 was the principal RNA found in VLP^{28H} virions of the faster sedimenting peak (Fig. 4C). Western blot analysis of viral CP in all three peaks was indistinguishable from that of wt BMV, suggesting that no modifications to BMV CP expressed from 30B-BCP had occurred (data not shown).

Assembly in Vitro of VLP^{28} and VLP^{22} Virions. Bromoviruses can readily be assembled *in vitro* from CP and RNA (*5, 15*). Whether the polymorphic nature associated with 30B-BCP infection *in vivo* can be mimicked *in vitro* was examined by providing the subgenomic RNAs of the hybrid virus as substrates. For this purpose, we constructed three independent plasmids from which RNA

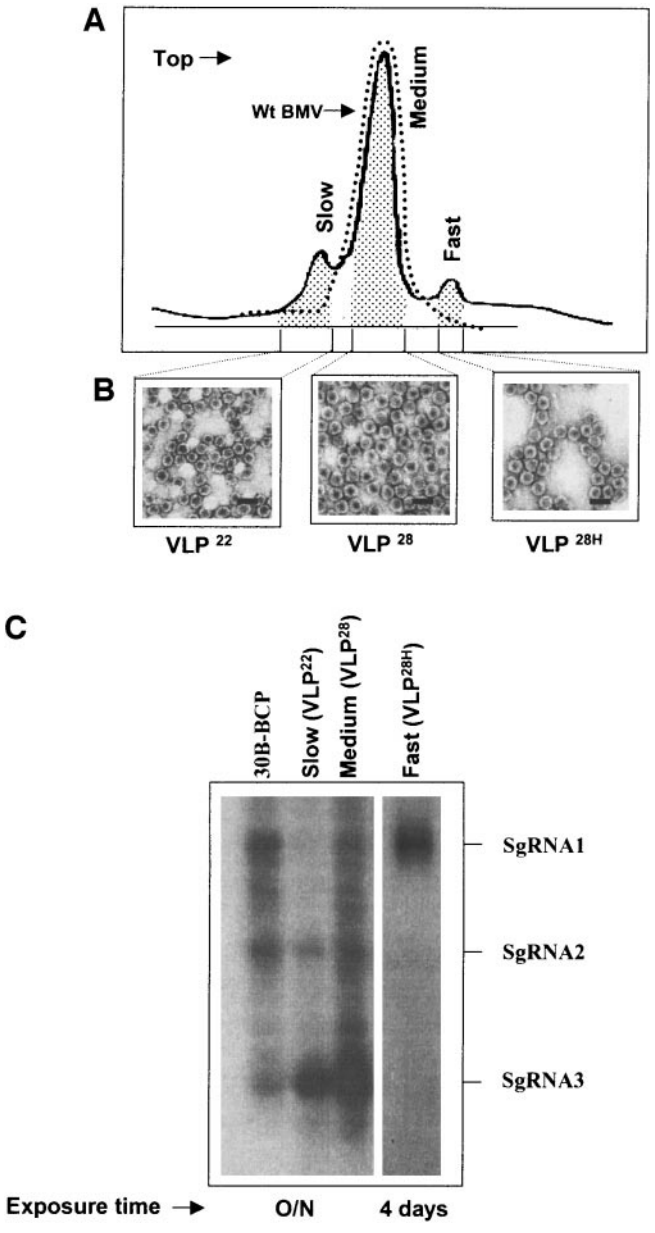

FIG. 4. Analysis of VLPs recovered from 30B-BCP infection. (A) Sucrose density gradient sedimentation analysis of partially purified virions of wt BMV (upper curve with dotted lines) and VLPs of 30B-BCP (lower curve). Resuspended partially purified preparations were subjected to centrifugation through a 10–40% linear sucrose gradient. Control purified preparations of wt BMV sedimented as a single peak (upper curve with dotted line) while those of 30B-BCP sedimented as slow, medium, and fast. Fractions corresponding to the shaded areas of each peak were pooled and concentrated by further high-speed centrifugation. (B) Electron micrographic images showing the negatively stained VLPs recovered from each of the three peaks of sucrose gradients as shown in A. Fractions constituting the slow sedimenting peak contained VLPs measuring 22–24 nm in diameter (VLP^{22}); fractions constituting the medium sedimenting peak contained VLPs measuring 28 nm in diameter (VLP^{28}); and fractions constituting the fast sedimenting peak contained VLPs measuring 28 nm in diameter (VLP^{28H}). Bar = 50 nm. (C) Northern blot hybridization of RNA extracted from VLP^{22}, VLP^{28}, and VLP^{28H} following sucrose density gradient fractionation. RNA isolated from partially purified preparations of 30B-BCP was used a control. The blot was hybridized with ^{32}P-labeled riboprobe complementary to BMV CP sequences. The positions of the three subgenomic RNAs are shown to the right.

transcripts identical to three subgenomic RNAs found in 30B-BCP infections (Fig. 1C) can be transcribed *in vitro* (Fig. 5A). Wt BMV CP subunits were allowed to reassemble with either individual transcripts of the three subgenomic RNAs or other possible permutations. Final products of each *in vitro* reassembly reaction were subjected to electron microscopic examination followed by quantitative analyses. Results of these experiments are summarized in Fig. 5. As reported earlier (*15*), under the conditions tested, the interaction between BMV CP and a given RNA was found to be highly specific since virion assembly occurred only when either virion RNA of 30B-BCP (Fig. 5A) or the transcripts of each of the three subgenomic RNAs of 30B-BCP (Figs. 5B and 5C), but not control *Xenopus* RNA (Fig. 5A), were provided as substrates. The most striking feature of *in vitro* reassembly assays is the ability of BMV CP to mimic polymorphism similar to that observed *in vivo* (Fig. 2A), except when SgRNA 1 alone was supplied as substrate (Fig. 5A). $VLPs^{22}$ were consistently observed in all other assay reactions and their proportions never exceed 14% of the total virion population. This polymorphism was observed only with subgenomic RNAs of 30B-BCP but not with wt BMV RNAs. It is significant to note that even transcripts of wt BMVRNA4, which is only 33 nt longer than SgRNA 3 (Fig. 1C), failed to display any polymorphism and always resulted in the assembly of VLP^{28} (Fig. 5A; *5*). These observations, together with the fact that BMV CP can assemble SgRNAs 2 and 3 into VLP^{22} (Fig. 4D), suggest that the observed polymorphism is not restricted by the size of the RNA but is controlled by a yet to be identified sequence and/or structural feature of the genetically modified subgenomic RNAs of the hybrid virus.

Results of this study exemplify some novel aspects relating to the assembly of BMV CP that have not been observed prior to this study. Expression of BMV CP from a TMV-based vector, independent of homologous replication machinery, had resulted in selective packaging of the three subgenomic RNAs generated from replication of the hybrid virus. This result is some what unexpected and intriguing, since BMV CP had been shown to exhibit a high degree of specificity in packaging both *in vitro* and *in vivo* (*13, 14*). The origin of assembly sequences in BMV is not known. Thus, reasons for the observed heterologous packaging by BMV CP are currently obscure. However, efficient packaging of subgenomic RNAs by BMV CP suggests that some features present in hybrid virus sequence are recognized by BMV CP subunits during assembly. In BMV, postulated copackaging of BMV RNAs 3 and 4 into one particle suggest that the CP sequence common to these two RNAs is likely to contain the origin of assembly. Therefore, one possible explanation for the observed heterologous packaging in this study is that the BMV CP sequence present at the 3′ half of each of the three subgenomic RNAs of the hybrid (Fig. 1B) could possibly mediate RNA packaging. However, available evidence suggests that this may not be the case. For

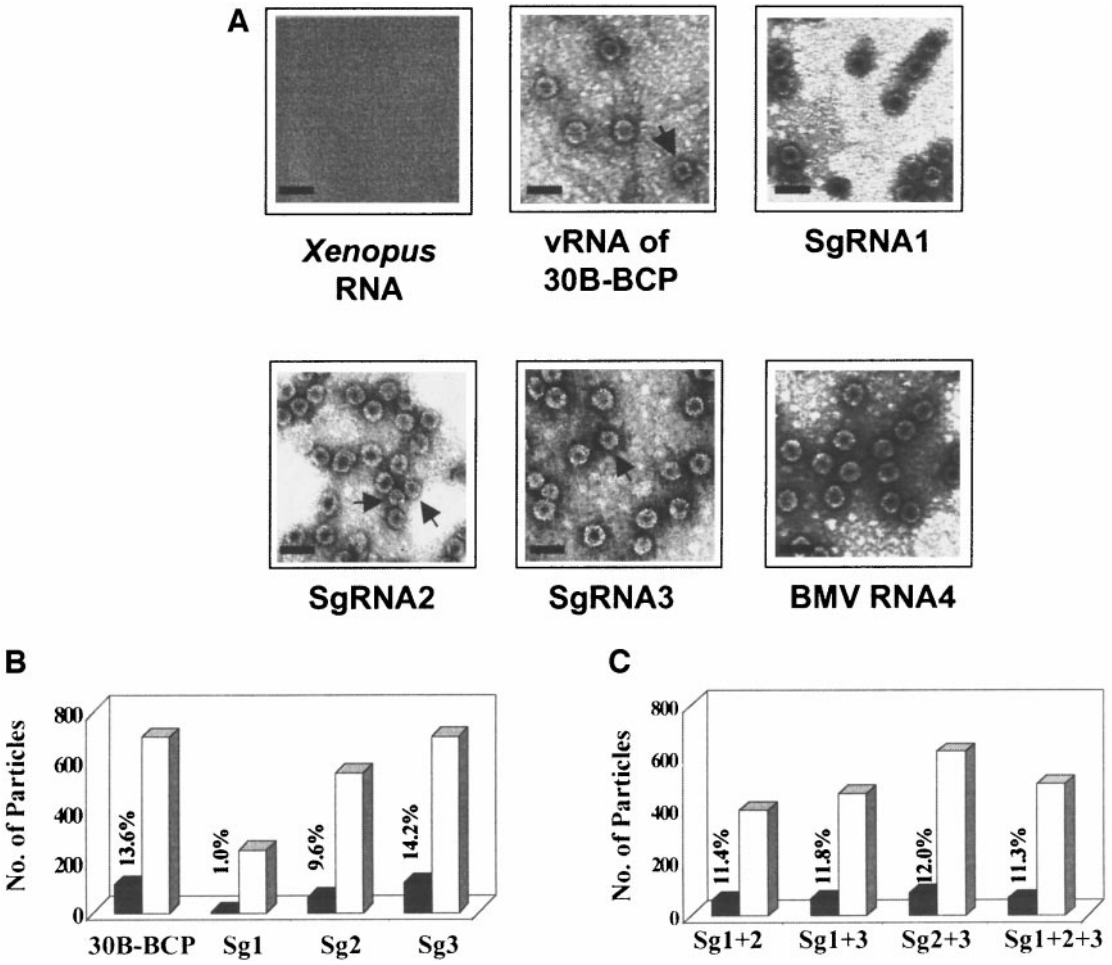

FIG. 5. *In vitro* reassembly assays. (A) Electron micrographs of negatively stained VLPs resulting from *in vitro* reassembly assays. Purified BMV CP subunits and the indicated RNAs were allowed to reassemble as described under Materials and Methods. Arrow indicates VLP^{22}. Bar = 50 nm. (B and C) Quantitative analysis of VLP^{22} and VLP^{28} assembled *in vitro.* Purified wt BMV CP subunits were allowed to assemble *in vitro* with virion RNA of 30B-BCP or the indicated single (B) or desired combinations (C) of each of the three subgenomic RNAs synthesized from the respective transcriptional plasmids (Fig. 1C). Filled and open bars represent VLP^{22} and VLP^{28}, respectively. The percentage of VLP^{22} among the total population of VLPs assembled is shown. An area measuring 7.5 μm^2 on each electron micrographic negative taken at 50 K was used to visually count the different-size VLPs and the data shown are an average of three independent experiments.

example, BMV CP expressed via subgenomic RNA of *cucumber mosaic virus* (a tripartite RNA virus similar in genome organization to BMV) was unable to package the chimeric RNA harboring BMV CP sequences (*14*). Therefore, sequence and/or structural features other than BMV CP sequences (for example, 3′ tRNA-like structures) common to all three subgenomic RNAs of the hybrid virus could play an important role in promoting the virion assembly by BMV CP subunits.

Another significant outcome of this study is the ability of BMV CP subunits to assemble into two distinct-size capsids *in vivo* and *in vitro.* Prior to this study, Kroll *et al.* (*16*) reported that BMV CP can assemble into a 120-subunit capsid with $T = 1$ symmetry, in addition to normal wt virions, when it was expressed in a yeast-based system from a genetically modified CP mRNA. These 120-subunit capsids exhibited features, such as size of the virions and sedimentation profile in sucrose density gradients, identical to those of VLP^{22} resulting from 30B-BCP infection observed in this study (Fig. 4A). Based on this analogy, we predict that VLP^{22} found in the purified preparations of 30B-BCP (Fig. 2A) as well as in our *in vitro* reassembly assays (Fig. 5A) are likely to be assembled from 120-CP subunits with $T = 1$ symmetry. Finally, our ability to reassemble both VLP^{22} and VLP^{28} *in vitro* by providing subgenomic RNA transcripts individually or in a desired combination will help in characterizing polymorphic forms assembled from BMV CP. Additional physical properties of VLP^{22}, VLP^{28}, and VLP^{28H} followed by cryoelectron microscopy and three-dimensional image reconstitution experiments are likely to shed more light on the assembly of icosahedral virions of RNA viruses.

Materials and Methods. Construction of a TMV hybrid vector expressing BMV CP. A TMV-based vector (p30B), designed for foreign gene expression, was constructed from parts of U1 and *Tobacco mild green mosaic virus*

(TMGMV) strain U5 (Fig. 1A; *9*). A sequence encoding BMV CP open reading frame (ORF) was PCR amplified from the pT7B3 (*17*) using a 5′ terminal (5′ GGCCTTAATTAAATGTCGACTTCAGGAACTGG 3′; *Pac*I site is underlined) and a 3′ terminal (5′ GTCGGCCTCGAGCTACCTATAAAGCGGGGTGAAG 3′; *Xho*I site is underlined) primer. This fragment was digested with *Pac*I and *Xho*I and ligated into similarly treated p30B yielding p30B-PX. The entire 3′ proximal sequence encompassing the TMGMV U5 CP ORF and its nontranslated region (3′ NTR) was deleted from p30B-PX as a *Pml*I (located in the TMV U1 NTR downstream of the foreign gene insertion site of p30B) and *Kpn*I (located at the end of p30B) fragment and replaced with another *Pml*I and *Kpn*I fragment encompassing the entire U1 3′ NTR yielding a recombinant plasmid p30B-BCP (Fig. 1B). The presence of the BMV CP ORF sequence in p30B-BCP was analyzed by restriction mapping and DNA sequencing.

Construction of in Vitro Transcriptional Plasmids for 30B-BCP Subgenomic RNAs. Three plasmids, pSgRNA 1, pSgRNA 2, and pSgRNA 3, respectively containing SgRNAs 1, 2, and 3 of 30B-BCP, were constructed as follows. DNA fragments encompassing the sequences of SgRNAs 1, 2, and 3 were independently amplified in a PCR reaction using a 5′ primer (for SgRNA 1, ^{3386}AGATATGTATAATCGCGATGCAGGAACACAATAGCA^{3421}, *Nru*I site is underlined; for SgRNA 2, ^{4876}AGTTCTTTTTAGGAATTCGTTTATAGATGGCTCTAG^{4912}, *Eco*RI site is underlined; for SgRNA 3, ^{5702}TCGCCGAATCGAATTCGTTTTAAATAGATCTTA^{5735}, *Eco*RI site is underlined) and a common 3′ primer (^{6556}ATCCGGGTACCTGGGCCGCTACCCGCGGTTAGGGGAGGATTC^{6515}, *Kpn*I site is underlined). After digesting each PCR fragment with the desired restriction enzymes (*Nru*I and *Kpn*I for SgRNA 1; *Eco*RI and *Kpn*I for SgRNAs 2 and 3), the fragments were ligated into a similarly treated pT7/T3-18U. *In vitro* transcription of each plasmid following linearization with *Kpn*I will result in the synthesis of respective subgenomic RNA transcripts (Fig. 1C) identical to those found in 30B-BCP infections (Fig. 1B).

In Vitro Transcription, Plant Inoculations, and Virus Purification. Procedures involving synthesis of infectious *in vitro* transcripts of BMV, TMV hybrid, inoculation of *Chenopodium quinoa* plants, characterization of progeny RNA, and coat protein by Northern and Western blots, respectively, were as described previously (*15, 17, 18*). Virions were purified from symptomatic leaves and treated with ribonuclease and RNA was isolated using SDS–phenol (*18*).

Riboprobe Synthesis. A T7 RNA polymerase transcript of pT7T3B3SB was used to detect progeny RNA 3 and 4 of BMV (*14*). A T7 RNA polymerase transcript from pT7T3/TMV54k, constructed by cloning a PCR product encompassing a sequence encoding TMV U1 54-kDa replicase gene (bases 3405–4254) into pT7/T3-18U, was used to detect (+) strand 54-kDa subgenomic RNA. A T7 RNA polymerase transcript from pT7T3/TMV-MP, constructed by cloning a PCR product encompassing a sequence encoding TMV U1 MP gene (bases 4888–5702) into pT7/T3-18U, was used to detect (+) strand MP subgenomic RNA. A T7 RNA polymerase transcript from pT7T3/U1 CP, constructed by cloning a PCR product encompassing a sequence encoding U1 CP (bases 5785–6056) into pT7/T3-18U, was used to detect (+) strand U1 CP subgenomic RNA.

Coat Protein Preparation, in Vitro Reassembly Assays, and Electron Microscopy. Isolation of viral coat protein subunits from purified virions and conditions used for *in vitro* reassembly are as described previously (*15, 19*). *In vitro* reassembled virions were negatively stained with 1% uranyl acetate and examined under a Hitachi transmission electron microscope.

ACKNOWLEDGMENTS

We thank Greg Pogue for providing us with the TMV-based vectors, Jack Johnson and Anthony Clark for helpful discussions, and George Grantham for excellent technical assistance in making several plasmid constructs. This research was supported by grants from USDA NRICP (9935303) and Academic Senate, University of California at Riverside.

REFERENCES

1. Ahlquist, P. (1994). Bromoviruses. *In* "Encyclopedia of Virology" (R. G. Webster and A. Granoff, Eds.), Vol. 1, pp. 181–185. Academic Press, San Diego.
2. Kao, C. C., Quadt, R., Hershberger, R. P., and Ahlquist, P. (1992). Brome mosaic virus RNA replicase proteins 1a and 2a from a complex *in vitro*. *J. Virol.* **66,** 6322–6329.
3. Lewandowski, D. J., and Dawson, W. O. (1999). Tobamoviruses. *In* "Encyclopedia of Virology," 2nd ed. (A. Granoff and R. G. Webster, Eds.), Vol 3, pp. 1780–1783. Academic Press, San Diego.
4. Zaitlin, M. (1999). Elucidation of the genome organization of tobacco mosaic virus. *Phil. Trans. R. Soc. Lond. B.* **354,** 587–591.
5. Fox, J. M., Johnson, J. E., and Young, M. (1994). RNA/protein interactions in icosahedral virus assembly. *Semin. Virol.* **5,** 51–60.
6. Beachy, R. N., Zaitlin, M., Bruening, G., and Israel, H. W. (1976). A genetic map for the cowpea strain of TMV. *Virology* **73,** 498–507.
7. Okada, Y. (1999). Historical overview of research on the tobacco mosaic virus genome: Genome organization, infectivity and gene manipulation. *Phil. Trans. R. Soc. Lond. B.* **354,** 569–582.
8. Pogue, G. P., Lindbo, J. A., Dawson, W. O., and Turpen, T. H. (1998). Tobamovirus transient expression vectors: tools for plant biology and high-level expression of foreign proteins in plants. *In* "Plant Molecular Biology Manual" (S. B. Gelvin and A. Schilperoort, Eds.) L4, pp 1–27. Kulwer Academic, Dordrecht, The Netherlands.
9. Shivaprasad, S., Pogue, G. P., Lewandowski, D. J., Hidalgo, J., Donson, J., Grill, L. K., and Dawson, W. O. (1999). Heterologous sequences greatly affect foreign gene expression in tobacco mosaic virus-based vectors. *Virology* **255,** 312–323.
10. Rao, A. L. N., and Grantham, G. L. (1995). Biological significance of the seven amino-terminal basic residues of brome mosaic virus coat protein. *Virology* **211,** 42–52.
11. Deom, C. M., Shaw, M. J., and Beachy, R. N. (1987). The 30-kilo Dalton gene product of tobacco mosaic virus potentiates virus movement. *Science* **249,** 1044–1046.
12. Schmitz, I., and Rao, A. L. N. (1996). Molecular studies on bromo-

virus capsid protein. I. Characterization of cell-to-cell defective RNA3 variants of brome mosaic virus. *Virology* **226,** 281–293.

13. Cuillel, M., Herzog, M., and Hirth, L. (1983). Specificity of *in vitro* reconstruction of bromegrass mosaic virus. *Virology* **95,** 146–153.

14. Osman, F., Choi, Y. G., Grantham, G. L., and Rao, A. L. N. (1998). Molecular studies on brome mosaic virus coat protein. V. Evidence for the specificity of brome mosaic virus encapsidation using RNA3 chimera of brome mosaic and cucumber mosaic viruses expressing heterologous coat proteins. *Virology* **251,** 438–448.

15. Choi, Y. G., Grantham, G. L., and Rao, A. L. N. (2000). Molecular studies on bromovirus capsid protein. VI. Contributions of the N-terminal arginine rich motif of BMV capsid protein to virion stability and packaging. *Virology* **270,** 377–385.

16. Krol, M. A., Olson, N. H., Tate, J., Johnson, J. E., Baker, T. S., and Ahlquist, P. (1999). RNA-controlled polymorphism in the *in vivo* assembly of 180-subunit and 120-subunit virions from a single coat protein. *Proc. Natl. Acad. Sci. USA* **96,** 13650–13655.

17. Dreher, T. W., Rao, A. L. N., and Hall, T. C. (1989). Replication *in vivo* of mutant brome mosaic virus RNAs defective in aminoacylation. *J. Mol. Biol.* **206,** 425–438.

18. Rao, A. L. N., Duggal, R., Lahser, F., and Hall, T. C. (1994). Analysis of RNA replication in plant viruses. *In* "Methods in Molecular Genetics: Molecular Virology Techniques" (K. W. Adolph, Ed.), Vol. 4, pp. 216–236. Academic Press, Orlando.

19. Zhao, X., Fox, J. M., Olson, N. H., Baker, T. M., and Young, M. J. (1995). *In vitro* assembly of cowpea chlorotic mottle virus from coat protein expressed in *Escherichia coli* and *in vitro* transcribed viral cDNAs. *Virology* **207,** 486–494.